

PRODUCTION OF FORWARD CHARM AND NEUTRINOS, AND UNINTEGRATED GLUON DISTRIBUTIONS AT VERY SMALL x^*

ANTONI SZCZUREK^{a,b}, RAFAŁ MACIULA^a

^aInstitute of Nuclear Physics Polish Academy of Sciences
Radzikowskiego 152, 31-342 Kraków, Poland

^bCollege of Natural Sciences, Institute of Physics, University of Rzeszów
Pigonia 1, 35-310 Rzeszów, Poland

*Received 20 December 2022, accepted 16 January 2023,
published online 25 May 2023*

In this presentation, we discussed production of charm quarks and anti-quarks, D mesons, and neutrinos/antineutrinos in forward and very forward directions. Gluon–gluon fusions, intrinsic charm, and recombination mechanisms were included. The gluon–gluon contribution, as well as the intrinsic charm contribution, were calculated in the k_t and hybrid factorization, while the recombination contribution in the standard collinear approach. Different unintegrated gluon distributions from the literature were used. We compared the results of our calculations for D mesons with the LHCb data for different rapidity intervals. The best description was achieved for the Martin–Ryskin–Watt (MRW) uPDF. We presented also energy distributions for forward electron, muon, and tau neutrinos to be measured at the LHC by the currently operating $\text{FASER}\nu$ experiment, as well as by future experiments such as $\text{FASER}\nu 2$ or FLArE , proposed very recently by the Forward Physics Facility project. At very forward directions, the intrinsic charm and recombination contributions become very important. We presented also neutrino energy fluxes including the above-mentioned processes. For electron and muon neutrinos, intrinsic charm and recombination mechanisms lead to similar production rates and their separation seems rather impossible. On the other hand, for $\nu_\tau + \bar{\nu}_\tau$ neutrino flux, the recombination is further reduced making the measurement of the IC contribution very attractive.

DOI:10.5506/APhysPolBSupp.16.5-A23

1. Introduction

The dominant mechanism of charm production is gluon–gluon fusion. At high energy, this mechanism is known to dominate at midrapidity. On the

* Presented at the Diffraction and Low- x 2022 Workshop, Corigliano Calabro, Italy, 24–30 September, 2022.

other hand, the mechanism of the forward production is not well known. In this presentation, two new mechanisms are considered:

- (a) Intrinsic charm-induced mechanism,
- (b) Recombination mechanism.

Both mechanisms cannot be predicted from first principles. The results depend on some model parameters. The FASER ν project [1] will study the forward production of different kinds of neutrinos in proton–proton collisions at the LHC. Can such data provide new information on the not well known mechanisms? We will show the energy distributions of such neutrinos also here. This project is important for the production of high-energy neutrinos in the Earth’s atmosphere (IceCube).

2. Sketch of the formalism

In Fig. 1, we present the diagrams showing the k_t -factorization approach (see *e.g.* [2]) for $c\bar{c}$ production (left panel) and the hybrid approach [3] for the intrinsic charm contribution (right panel).

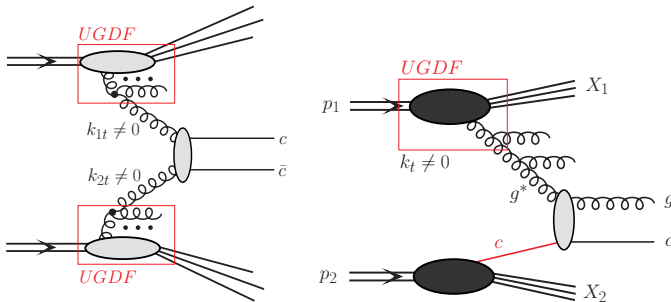


Fig. 1. The k_t -factorization approach for $c\bar{c}$ production (left) and the hybrid approach for the intrinsic charm contribution (right).

The cross section in the k_t -factorization approach is written as

$$\frac{d\sigma(pp \rightarrow c\bar{c}X)}{dy_1 dy_2 d^2p_{1,t} d^2p_{2,t}} = \int \frac{d^2k_{1,t}}{\pi} \frac{d^2k_{2,t}}{\pi} \frac{1}{16\pi^2(x_1 x_2 s)^2} \left| \overline{\mathcal{M}_{g^*g^* \rightarrow c\bar{c}}}^{\text{off-shell}} \right|^2 \times \delta^2(\vec{k}_{1,t} + \vec{k}_{2,t} - \vec{p}_{1,t} - \vec{p}_{2,t}) \mathcal{F}_g(x_1, k_{1,t}^2, \mu^2) \mathcal{F}_g(x_2, k_{2,t}^2, \mu^2), \quad (1)$$

where $\mathcal{F}_g(x_1, k_{1,t}^2, \mu^2)$ and $\mathcal{F}_g(x_2, k_{2,t}^2, \mu^2)$ are the gluon uPDFs for both colliding hadrons, and $\mathcal{M}_{g^*g^* \rightarrow c\bar{c}}^{\text{off-shell}}$ is the off-shell matrix element.

The longitudinal momentum fractions are calculated as

$$\begin{aligned} x_1 &= \frac{m_{1,t}}{\sqrt{s}} \exp(+y_1) + \frac{m_{2,t}}{\sqrt{s}} \exp(+y_2), \\ x_2 &= \frac{m_{1,t}}{\sqrt{s}} \exp(-y_1) + \frac{m_{2,t}}{\sqrt{s}} \exp(-y_2), \end{aligned} \quad (2)$$

where $m_{i,t} = \sqrt{p_{i,t}^2 + m_c^2}$ is the quark/antiquark transverse mass.

The intrinsic charm component is calculated in the hybrid approach as it was done in Refs. [4–6]. In this approach, the differential cross section for $pp \rightarrow gcX$ via $g^*c \rightarrow gc$ mechanism reads

$$d\sigma_{pp \rightarrow gcX} = \int d^2k_t \int \frac{dx_1}{x_1} \int dx_2 \mathcal{F}_{g^*}(x_1, k_t^2, \mu^2) c(x_2, \mu^2) d\hat{\sigma}_{g^*c \rightarrow gc}, \quad (3)$$

where $\mathcal{F}_{g^*}(x_1, k_t^2, \mu^2)$ is the unintegrated gluon distribution in one proton and $c(x_2, \mu^2)$ a collinear charm quark PDF in the second one. Here, we take the intrinsic charm distributions in the proton obtained according to the BHPS model [7]. The $d\hat{\sigma}_{g^*c \rightarrow gc}$ is the hard partonic cross section obtained from a gauge-invariant tree-level off-shell amplitude.

The recombination components shown in Fig. 2 are calculated in the collinear approach as it was done in Ref. [8]. The differential cross section for production of Dc final state reads

$$\begin{aligned} \frac{d\sigma}{dy_1 dy_2 d^2p_t} &= \frac{1}{16\pi^2 \hat{s}^2} \left[x_1 q_1(x_1, \mu^2) x_2 g_2(x_2, \mu^2) \overline{|\mathcal{M}_{qg \rightarrow Dc}(s, t, u)|^2} \right. \\ &\quad \left. + x_1 g_1(x_1, \mu^2) x_2 q_2(x_2, \mu^2) \overline{|\mathcal{M}_{gq \rightarrow Dc}(s, t, u)|^2} \right]. \end{aligned} \quad (4)$$

Above, y_1 is the rapidity of the D meson and y_2 the rapidity of the associated c quark or \bar{c} antiquark.

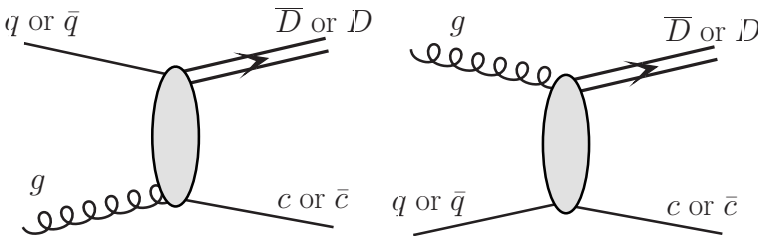


Fig. 2. Schematic diagrams for the recombination.

The matrix element squared in (4) can be written as

$$|\mathcal{M}_{qg \rightarrow Dc}(s, t, u)|^2 = |\mathcal{M}_{qg \rightarrow (\bar{c}q)^n c}|^2 \rho, \quad (5)$$

where n enumerates quantum numbers of the $\bar{c}q$ system $n \equiv {}^{2J+1}L$. The matrix elements were calculated by Braaten, Jia, Mehen [9–11] and ρ can be interpreted as a probability to form a real meson. For illustration, as our default set, we shall take $\rho = 0.1$, but the precise number should be adjusted to experimental data on D^0/\bar{D}^0 production asymmetry. We shall return to this point in the conclusion section. The factorization scale in the calculation is taken as $\mu^2 = p_t^2 + \frac{m_{t,D}^2 + m_{t,c}^2}{2}$.

3. Selected results

In Fig. 3, we show some examples of transverse momentum (left) and rapidity (right) distributions for $D^0 + \bar{D}^0$. The calculation was performed within the k_t -factorization approach. In these calculations, the unintegrated gluon densities from the MRW-MMHT2014nlo model [12] were used. Rather good agreement with the data was achieved. In Ref. [13], we showed also distributions for more forward rapidities.

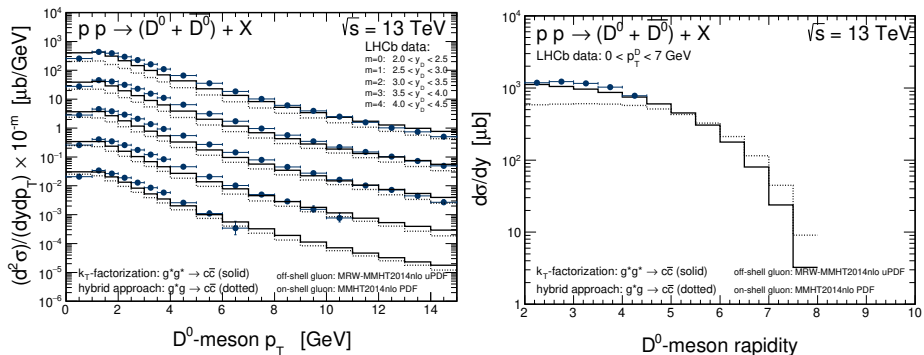


Fig. 3. An example for the D^0 production for the LHCb kinematics.

Below, we show also energy distributions of neutrinos (plus antineutrinos) coming from semileptonic decays of D mesons (see Figs. 4 and 5). As a reference, we show also the result of conventional component (decays of light mesons). In general, the decays of D mesons populate regions of larger neutrino energies. This is particularly true for intrinsic charm and recombination contributions. While for the electron neutrinos/antineutrinos the intrinsic charm and recombination contributions are of a similar order for the tau neutrinos/antineutrinos, the recombination contribution is much

smaller. This makes the measurement of tau neutrinos particularly promising in the context of searches for intrinsic charm. In Ref. [13], we show also the distribution of muon neutrinos/antineutrinos. There, the pion decay contribution is large which makes the searches for IC rather difficult.

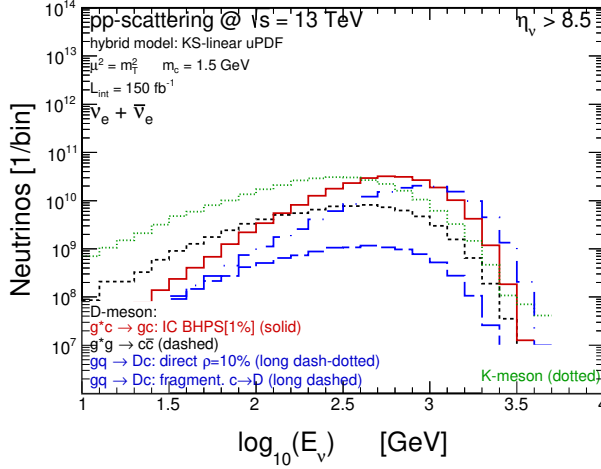


Fig. 4. Energy distribution of ν_e neutrinos.

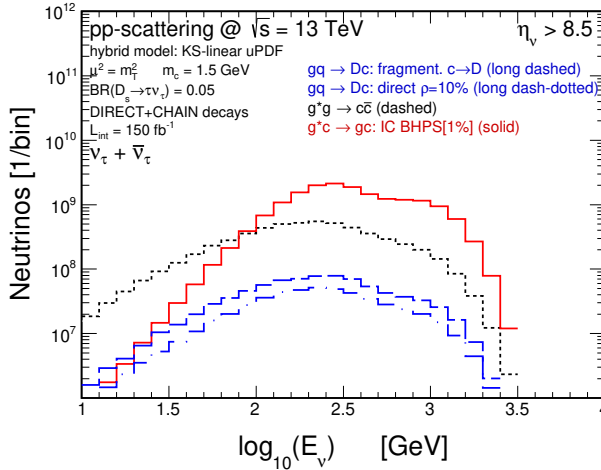


Fig. 5. Energy distribution of ν_τ neutrinos.

4. Conclusions

Here, we have discussed production of charmed quarks, mesons, and associated neutrinos/antineutrinos in proton–proton collisions. We have considered gluon–gluon fusion, intrinsic charm, and recombination contributions. Some parameters of the intrinsic charm model and recombination were fixed

from previous studies. The recombination parameter $\rho = 0.1$ is almost consistent with recent studies of asymmetry between the D^0 and \bar{D}^0 production in fixed target $p + {}^{20}\text{Ne}$ collisions [14].

We have calculated transverse momentum distributions of $D^0 + \bar{D}^0$ for different bins of meson rapidities. The results of the calculations have been compared to the LHCb experimental data. A very good agreement has been achieved for the Martin–Ryskin–Watt unintegrated gluon distribution. In the original paper [13] we presented also results for the Kutak–Sapeta unintegrated gluon distributions.

We have also presented energy distributions of neutrinos/antineutrinos from the decay of D mesons including all considered contributions. At the large neutrino energies, the intrinsic charm and recombination contributions play an important role. While for electron neutrinos/antineutrinos both intrinsic charm and recombination contributions are crucial, for tau neutrinos/antineutrinos, one has unique dominance of intrinsic charm contribution. This makes the measurement of tau neutrinos particularly valuable in searches for an intrinsic charm component.

This study was supported by the National Science Center, Poland (NCN) grant UMO-2018/31/B/ST2/03537 and the Center for Innovation and Transfer of Natural Sciences and Engineering Knowledge in Rzeszów.

REFERENCES

- [1] FASER Collaboration (H. Abreu *et al.*), *Eur. Phys. J. C* **80**, 61 (2020).
- [2] S. Catani, M. Ciafaloni, F. Hautmann, *Phys. Lett. B* **242**, 97 (1990); *Nucl. Phys. B* **366**, 135 (1991); *Phys. Lett. B* **307**, 147 (1993).
- [3] M. Deak *et al.*, *J. High Energy Phys.* **2009**, 121 (2009).
- [4] R. Maciuła, A. Szczurek, *J. High Energy Phys.* **2020**, 135 (2020).
- [5] R. Maciuła, A. Szczurek, *Phys. Rev. D* **105**, 014001 (2022).
- [6] V.P. Goncalves, R. Maciuła, A. Szczurek, *Eur. Phys. J. C* **82**, 236 (2022).
- [7] S.J. Brodsky *et al.*, *Phys. Lett. B* **93**, 451 (1980).
- [8] R. Maciuła, A. Szczurek, *Phys. Lett. B* **835**, 137530 (2022).
- [9] E. Braaten, Y. Jia, T. Mehen, *Phys. Rev. D* **66**, 034003 (2002).
- [10] E. Braaten, Y. Jia, T. Mehen, *Phys. Rev. Lett.* **89**, 122002 (2002).
- [11] E. Braaten, Y. Jia, T. Mehen, *Phys. Rev. D* **66**, 014003 (2002).
- [12] G. Watt, A.D. Martin, M.G. Ryskin, *Eur. Phys. J. C* **31**, 73 (2003).
- [13] R. Maciuła, A. Szczurek, *Phys. Rev. D* **107**, 034002 (2023), [arXiv:2210.08890](https://arxiv.org/abs/2210.08890) [hep-ph].
- [14] LHCb Collaboration, [arXiv:2211.11633](https://arxiv.org/abs/2211.11633) [hep-ex].